Observation of $K_s^0 K_s^0$ resonances in deep inelastic scattering at HERA

ZEUS Collaboration

Abstract

Inclusive $K_s^0 K_s^0$ production in deep inelastic ep scattering at HERA has been studied with the ZEUS detector using an integrated luminosity of 120 pb^{-1}. Two states are observed at masses of 1537^{+9}_{-8} MeV and 1726 ± 7 MeV, as well as an enhancement around 1300 MeV. The state at 1537 MeV is consistent with the well established $f_2'(1525)$. The state at 1726 MeV may be the glueball candidate $f_0(1710)$.

1 Introduction

The $K_s^0 K_s^0$ system is expected to couple to scalar and tensor glueballs. This has motivated intense experimental and theoretical study during the past few years [1,2]. Lattice QCD calculations [3] predict the existence of a scalar glueball with a mass of 1730 ± 100 MeV and a tensor glueball at 2400 ± 120 MeV. The scalar glueball can mix with $q\bar{q}$ states with $I = 0$ from the scalar meson nonet, leading to three $J^{PC} = 0^{++}$ states, whereas only two can fit into the nonet. Experimentally, four states with $J^{PC} = 0^{++}$ and $I = 0$ have been established [4]: $f_0(980)$, $f_0(1370)$, $f_0(1500)$ and $f_0(1710)$.

The state most frequently considered to be a glueball candidate is $f_0(1710)$ [4], but its gluon content has not yet been established. This state was first observed in radiative J/ψ decays [5] and its angular momentum $J = 0$ was established by the WA102 experiment using a partial-wave analysis in the K^+K^- and $K_s^0 K_s^0$ final states [6]. A recent publication from L3 [7] reports the observation of two states in $\gamma\gamma$ collisions above 1500 MeV, the well established $f_2'(1525)$ [4] and a broad resonance at 1760 MeV. It is not clear if this state is the $f_0(1710)$. Observation of $f_0(1710)$ in $\gamma\gamma$ collisions would indicate a large quark content.

The ep collisions at HERA provide an opportunity to study resonance production in a new environment. The production of K_s^0 has been studied previously at HERA [8,9]. In this paper, the first observation of resonances in the $K_s^0 K_s^0$ final state in inclusive ep deep inelastic scattering (DIS) is reported.

2 Experimental set-up

The data were collected by the ZEUS detector at HERA during the 96-00 running periods. In 96-97, HERA collided 27.5 GeV positrons with 820 GeV protons. In 98-00, the proton energy was 920 GeV and both positrons and electrons were collided with protons. The measurements for e^+p (e^-p) interactions[1] are based on an integrated luminosity of $104\,\mathrm{pb}^{-1}$ ($17\,\mathrm{pb}^{-1}$).

A detailed description of the ZEUS detector can be found elsewhere [10]. A brief outline of the components that are most relevant for this analysis is given below.

Charged particles are tracked in the central tracking detector (CTD) [11], which operates in a magnetic field of 1.43 T provided by a thin superconducting solenoid. The CTD consists of 72 cylindrical drift chamber layers, organized in nine superlayers covering the

[1] Hereafter, both e^+ and e^- are referred to as electrons, unless explicitly stated otherwise.

polar-angle[2] region $15^\circ < \theta < 164^\circ$. The relative transverse-momentum resolution for full-length tracks is $\sigma(p_T)/p_T = 0.0058 p_T \oplus 0.0065 \oplus 0.0014/p_T$, with p_T in GeV. The tracking system was used to establish the primary and secondary vertices.

The high-resolution uranium–scintillator calorimeter (CAL) [12] consists of three parts: the forward (FCAL), the barrel (BCAL) and the rear (RCAL) calorimeters. Each part is subdivided transversely into towers and longitudinally into one electromagnetic section (EMC) and either one (in RCAL) or two (in BCAL and FCAL) hadronic sections (HAC). The smallest subdivision of the calorimeter is called a cell. The CAL energy resolutions, as measured under test-beam conditions, are $\sigma(E)/E = 0.18/\sqrt{E}$ for electrons and $\sigma(E)/E = 0.35/\sqrt{E}$ for hadrons, with E in GeV.

The energy of the scattered electron was corrected for energy loss in the material between the interaction point and the calorimeter using a small-angle rear tracking detector (SRTD) [13, 14] and a presampler (PRES) [14, 15].

3 Kinematic reconstruction and event selection

The inclusive neutral current DIS process $e(k) + p(P) \rightarrow e(k') + X$ can be described in terms of the following variables: the negative of the invariant-mass squared of the exchanged virtual photon, $Q^2 = -q^2 = -(k - k')^2$; the fraction of the lepton energy transferred to the proton in the proton rest frame, $y = (q \cdot P)/(k \cdot P)$; and the Bjorken scaling variable, $x = Q^2/(2P \cdot q)$.

A three-level trigger system was used to select events online [10]. The inclusive DIS selection was defined by requiring an electron found in the CAL. In certain run periods, corresponding to 83% of the total luminosity, the inclusive selection was not available for low Q^2 ($Q^2 < 20$ GeV^2) events. For these periods, an additional selection with a requirement of at least one forward jet identified with the k_t algorithm [16] and having transverse energy $E_T > 3$ GeV ($E_T > 4$ GeV in the 2000 running period), pseudorapidity $0 < \eta_{\rm jet} < 3$ ($1.5 < \eta_{\rm jet} < 3.5$ in the 1996-1997 running period) was used.

The DIS offline event selection was based on the following requirements:

- a primary vertex position, determined from the tracks fitted to the vertex, in the range $\mid Z_{\rm vertex} \mid < 50$ cm, to reduce the background events from non-ep interactions;
- $E_e \geq 8.5$ GeV, where E_e is the energy of the scattered electron reconstructed in the calorimeter;

[2] The ZEUS coordinate system is a right-handed Cartesian system, with the Z axis pointing in the proton beam direction, referred to as the "forward direction", and the X axis pointing left towards the centre of HERA. The coordinate origin is at the nominal interaction point.

- $42 < \delta < 60$ GeV, where $\delta = \sum E_i(1 - \cos\theta_i)$, E_i is the energy of the i^{th} calorimeter cell and θ_i is its polar angle as viewed from the primary vertex. The sum runs over all cells. This cut further reduces the background from photoproduction and events with large QED initial-state radiation;
- $y_{\rm e} \leq 0.95$, to remove events with misidentified scattered DIS electrons; $y_{\rm e}$ is the value of y reconstructed using the scattered electron measurements;
- $y_{\rm JB} \geq 0.04$, to remove events with low hadronic activities; $y_{\rm JB}$ is the value of y reconstructed using the Jaquet-Blondel method [17];
- the position of the scattered lepton candidate in the RCAL was required to be outside a box of ± 14 cm in X and Y, which corresponds approximately to $\theta_{\rm ele} \approx 176^o$, where $\theta_{\rm ele}$ is the polar angle of the scattered electron;
- a maximum of 40 tracks per event. This cut reduces the background from false K^0_s pair candidates, removing only 7% of the DIS events.

The non-ep and photoproduction background in the selected sample was negligible. The data were not corrected for the biases introduced by the trigger requirements and selection cuts.

4 Selection of K^0_s-pair candidates

The K^0_s meson candidates were reconstructed using tracks with at least 38 hits in the CTD and pseudorapidity within ± 1.75. The pseudorapidity cut and the required minimum number of hits ensured a good momentum resolution and a minimum transverse momentum of 0.1 GeV. In each event, oppositely charged track pairs assigned to a secondary vertex were combined to form K^0_s candidates. Both tracks were assigned the mass of a charged pion and the invariant-mass $M(\pi^+\pi^-)$ calculated. The secondary vertex resolution for these events, estimated using MC studies, is 2 mm in X and Y, and 4 mm in Z.

Additional requirements were applied to the selected K^0_s candidates:

- $p_T(K^0_s) > 200$ MeV, for each K^0_s candidate;
- $2 < d < 30$ cm, where d is the decay length of the K^0_s candidate;
- $d_{XY} < 4$ mm and $d_Z < 5.5$ mm, where d_{XY} and d_Z are, respectively, the projections on the XY plane and Z axis of the vector defined by the primary interaction point and the point of closest approach of the K^0_s candidate;

- $\theta_{XY} < 0.12$, where θ_{XY} is the (collinearity) angle between the candidate K_s^0 momentum vector and the vector defined by the interaction point and the K_s^0 decay vertex in the XY plane;
- $p_T^A > 110$ MeV, for each K_s^0 candidate, where the Armenteros-Podolanski variable p_T^A is the projection of the candidate pion momentum onto a plane perpendicular to the K_s^0 candidate line of flight [18].

The cuts on the decay length, distance of closest approach and collinearity angle significantly reduce the non-K_s^0 background as determined by Monte Carlo (MC) simulations. After the p_T^A cut, backgrounds from Λ, $\overline{\Lambda}$ and photon conversions are negligible. Only events with at least two selected K_s^0 candidates were kept for further analysis.

Figure 1 shows the invariant-mass distribution for K_s^0 candidates in the range $0.45 < M(\pi^+\pi^-) < 0.55$ GeV after the K_s^0-pair candidate selection. The distribution was fitted using one linear and two Gaussian functions. The linear function fits the background, one of the Gaussians fits the peak region in the central $\pi^+\pi^-$ invariant mass distribution, and the other Gaussian improves the fit at the tails. The two Gaussians were constrained to have the same mean value. A mass of 498 MeV and standard deviation width of 4 MeV were obtained from the fit with the central Gaussian, and a standard deviation width of 8.5 MeV was obtained from the fit with the other Gaussian. The normalization factor between the narrower and broader Gaussians is approximately 5.5. The invariant-mass width is dominated by the momentum resolution of tracks reconstructed with the CTD. Only K_s^0 candidates in the region of ± 10 MeV around the fitted central mass were used to reconstruct the $K_s^0 K_s^0$ invariant-mass.

Figure 2 shows the distribution in x and Q^2 of selected events containing at least one pair of K_s^0 candidates. The kinematic variables were reconstructed using the double angle method [19]. The virtual-photon proton centre-of-mass energy was in the range $50 < W < 250$ GeV.

5 Results

The $K_s^0 K_s^0$ spectrum may have a strong enhancement near the $K_s^0 K_s^0$ threshold due to the $f_0(980)/a_0(980)$ state [20, 21]. Since the high $K_s^0 K_s^0$ mass is the region of interest for this analysis, the complication due to the threshold region is avoided by imposing the cut $cos\theta_{K_s^0 K_s^0} < 0.92$, where $\theta_{K_s^0 K_s^0}$ is the opening angle between the two K_s^0 candidates in the laboratory frame.

After applying all selections, 2553 K_s^0-pair candidates were found in the range $0.995 < M(K_s^0 K_s^0) < 2.795$ GeV, where $M(K_s^0 K_s^0)$ was calculated using the K_s^0 mass of 497.672 MeV

[4]. The momentum resolution of the CTD leads to an average $M(K_s^0K_s^0)$ resolution which ranges from 7 MeV in the 1300 MeV mass region to 10 MeV in the 1700 MeV region. Figure 3 shows the measured $K_s^0K_s^0$ invariant-mass spectrum. Two clear peaks are seen, one around 1500 MeV and the other around 1700 MeV, along with an enhancement around 1300 MeV. The data for $\cos\theta_{K_s^0K_s^0} > 0.92$ are also shown.

The distribution of Fig. 3 was fitted using three modified relativistic Breit-Wigner (MRBW) distributions and a background function $U(M)$;

$$F(M) = \sum_{i=1}^{3}\left(\frac{m_{*,i}\Gamma_{d,i}}{(m_{*,i}^2 - M^2)^2 + m_{*,i}^2\Gamma_{d,i}^2}\right) + U(M)\ , \qquad (1)$$

where $\Gamma_{d,i}$ is the effective resonance width, which takes into account spin and large width effects [22], $m_{*,i}$ is the resonance mass, and M is $K_s^0K_s^0$ invariant mass. The background function is

$$U(M) \ = \ A\cdot(M - 2m_{K_s^0})^B \cdot e^{-C\sqrt{M-2m_{K_s^0}}}\ , \qquad (2)$$

where A, B and C are free parameters and $m_{K_s^0}$ is the K_s^0 mass defined by Hagiwara et al [4].

Below 1500 MeV, a region strongly affected by the $\cos\theta_{K_s^0K_s^0}$ cut, a peak is seen around 1300 MeV where a contribution from $f_2(1270)/a_2^0(1320)$ is expected. This mass region was fitted with a single Breit-Wigner.

Above 1500 MeV, the lower-mass state has a fitted mass of 1537^{+9}_{-8} MeV and a width of 50^{+34}_{-22} MeV, in good agreement with the well established $f_2'(1525)$. The higher-mass state has a fitted mass of 1726 ± 7 MeV and a width of 38^{+20}_{-14} MeV. The widths reported here were stable, within statistical errors, to a wide variation of fitting methods. The width is narrower than the PDG value (125 ± 10 MeV) [4] reported for $f_0(1710)$, but when it is fixed to this value, the fit is still acceptable. For the purposes of the following discussion, this state is referred to as $f_0(1710)$.

The masses, widths and number of events from the fit with statistical errors are given in the top row of Table 1. The mass spectrum is also consistent with the background function at higher masses, but masses above 2.795 GeV were not included in the fit due to limited statistics. The sensitivity of the data to the widths of the resonances was studied. Several fits were performed fixing the width of the states $f_2'(1525)$ and $f_0(1710)$ to their PDG values; the results are shown in rows 2 to 4 of Table 1.

In the literature, there are several states reported in the mass region near 2 GeV [4], namely $f_2(1950)$ and $f_0(2020)$ which need confirmation, and $f_2(2010)$, $a_4(2040)$ and

$f_4(2050)$ which have been confirmed. The effect of the inclusion of a state in this region was examined, with the result shown in row 5 of Table 1.

The $K_s^0 K_s^0$ spectrum after all cuts was also fitted with the background function only. The fit can be rejected with a 99.4% confidence level using a χ^2 test.

It was found that 93% of the K_s^0-pair candidates selected within the detector and trigger acceptance are in the target region of the Breit frame [23], the hemisphere containing the proton remnant. Of the K_s^0-pair candidates in the target region, 78% are in the gluon-rich region $x_p = 2p_B/Q > 1$, where p_B is the absolute momentum of the $K_s^0 K_s^0$ in the Breit frame.

6 Conclusions

The first observation in *ep* deep inelastic scattering of a state at 1537 MeV, consistent with $f_2'(1525)$, and another at 1726 MeV, close to $f_0(1710)$, is reported. There is also an enhancement near 1300 MeV which may arise from the production of $f_2(1270)$ and/or $a_2^0(1320)$ states. The width of the state at 1537 MeV is consistent with the PDG value for the $f_2'(1525)$. The state at 1726 MeV has a mass consistent with the glueball candidate $f_0(1710)$, and is found in a gluon-rich region of phase space. However, it's width of 38^{+20}_{-14} MeV is narrower than the PDG value of 125 ± 10 MeV for the $f_0(1710)$.

7 Acknowledgements

We thank the DESY directorate for their strong support and encouragement. The special efforts of the HERA machine group in the collection of the data used in this paper are gratefully acknowledged. We are grateful for the support of the DESY computing and network services. The design, construction and installation of the ZEUS detector have been made possible by the ingenuity and effort of many people from DESY and home institutes who are not listed as authors. We also thank F. Close, S. Godfrey and H. Lipkin for their valuable comments and advice.

References

[1] S. Godfrey and J. Napolitano, Review of Modern Physics 71 (1999) 1411.

[2] E. Klempt, *Proc. of the PSI Zuoz Summer School on Phenomenology of Gauge Interactions*, p. 61. (2000). Also in preprint hep-ex/0101031.

[3] C. J. Morningstar and M. Peardon, Phys. Rev. D 60 (1999) 034509;
C. Michael and M. Teper, Nucl. Phys. B 314 (1989) 347.

[4] Particle Data Group, K. Hagiwara et al., Phys. Rev. D 66 (2002) 1.

[5] BES Collaboration, J. Z. Bai et al., Phys. Rev. Lett. 77 (1996) 3959.

[6] WA102 Collaboration, D. Barberis et al., Phys. Lett. B 453 (1999) 305.

[7] L3 Collaboration, M. Acciari et al., Phys. Lett. B 501 (2001) 173.

[8] ZEUS Collaboration, M. Derrick et al., Z. Phys. C 68 (1995) 29;
ZEUS Collaboration, J. Breitweg et al., Eur. Phys. J. C 2 (1998) 77.

[9] H1 Collaboration, S. Aid et al., Nucl. Phys. B 480 (1996) 3;
H1 Collaboration, C. Adloff et al., Z. Phys. C 76 (1997) 213.

[10] ZEUS Collaboration, U. Holm (ed.), *The ZEUS Detector*. Status Report (unpublished), DESY (1993), available on
`http://www-zeus.desy.de/bluebook/bluebook.html`.

[11] N. Harnew et al., Nucl. Inst. Meth. A 279 (1989) 290;
B. Foster et al., Nucl. Phys. Proc. Suppl. B 32 (1993) 181;
B. Foster et al., Nucl. Inst. Meth. A 338 (1994) 254.

[12] M. Derrick et al., Nucl. Inst. Meth. A 309 (1991) 77;
A. Andresen et al., Nucl. Inst. Meth. A 309 (1991) 101;
A. Caldwell et al., Nucl. Inst. Meth. A 321 (1992) 356;
A. Bernstein et al., Nucl. Inst. Meth. A 336 (1993) 23.

[13] A. Bamberger et al., Nucl. Inst. Meth. A 401 (1997) 63.

[14] ZEUS Collaboration, S. Chekanov et al., Eur. Phys. J. C 21 (2001) 443.

[15] A. Bamberger et al., Nucl. Inst. Meth. A 382 (1996) 419.

[16] S. Catani et al., Nucl. Phys. B 406 (1993) 187.

[17] F. Jacquet and A. Blondel, *Proc. of the Study for an ep Facility for Europe*, p. 391. Hamburg, Germany (1979).

[18] J. Podolanski and R. Armenteros, Phil. Mag 45 (1954) 13.

[19] S. Bentvelsen, J. Engelen and P. Kooijman, *Proc. Workshop on Physics at HERA*, Vol. 1, p. 23. Hamburg, Germany, DESY (1992).

[20] S. Godfrey and N. Isgur, Phys. Rev. D32 (1985) 189.

[21] WA102 Collaboration, D. Barberis et al., Phys. Lett. B 489 (2000) 24;
T. Barnes, *IX International Conference on Hadron Spectroscopy*, AIP Conference Proc. Vol. 619, p. 447. Protvino, Russia (2002). Also in preprint hep-ph/0202157.

[22] J. Benecke and H. P. Dürr, Nuovo Cimento 56 (1968) 269.

[23] R. P. Feynman, *Photon-Hadron Interactions*, Benjamin, New York (1972);
K.H. Streng, T.F. Walsh and P.M. Zerwas, Z. Phys. C 2 (1979) 237.

Fit	χ^2/N	$f_2(1270)/a_2^0(1320)$			$f_2'(1525)$			$f_0(1710)$			$f_J(1980)$		
		mass	width	events	mass	width	events	mass	width	events	mass	width	events
1	0.97	1274^{+17}_{-16}	244^{+85}_{-58}	414^{+184}_{-125}	1537^{+9}_{-8}	50^{+34}_{-22}	84^{+41}_{-31}	1726 ± 7	38^{+20}_{-14}	74^{+29}_{-23}			
2	0.96	1272 ± 16	240^{+76}_{-55}	420^{+167}_{-122}	1539 ± 10	76	107 ± 30	1727 ± 7	39 ± 20	76^{+28}_{-24}			
3	1.02	1276 ± 16	258^{+80}_{-59}	480^{+190}_{-141}	1536 ± 8	49^{+30}_{-21}	85^{+38}_{-27}	1726 ± 13	125	122 ± 40			
4	1.02	1274 ± 15	251^{+72}_{-55}	476^{+176}_{-131}	1538 ± 10	76	108^{+31}_{-29}	1728 ± 13	125	120^{+41}_{-38}			
5	1.00	1283 ± 15	260^{+70}_{-55}	506^{+218}_{-122}	1540^{+12}_{-10}	70^{+43}_{-30}	116^{+59}_{-42}	1727 ± 7	47^{+23}_{-15}	91^{+34}_{-26}	1970^{+33}_{-45}	138^{+173}_{-89}	74 ± 40
Particle Data Group 2002 Values (MeV) [4]													
		1275.5 ± 1.2, $185^{+3.4}_{-2.6}$ 1318 ± 0.6, 104.7 ± 1.9			1525 ± 5, 76 ± 10			1713 ± 6, 125 ± 10					

Table 1: *Normalized χ^2, masses in MeV, widths in MeV, and number of events extracted from the $K_s^0 K_s^0$ invariant mass fits (errors are statistical only.) Widths reported without errors were fixed to the PDG values listed in the last row.*

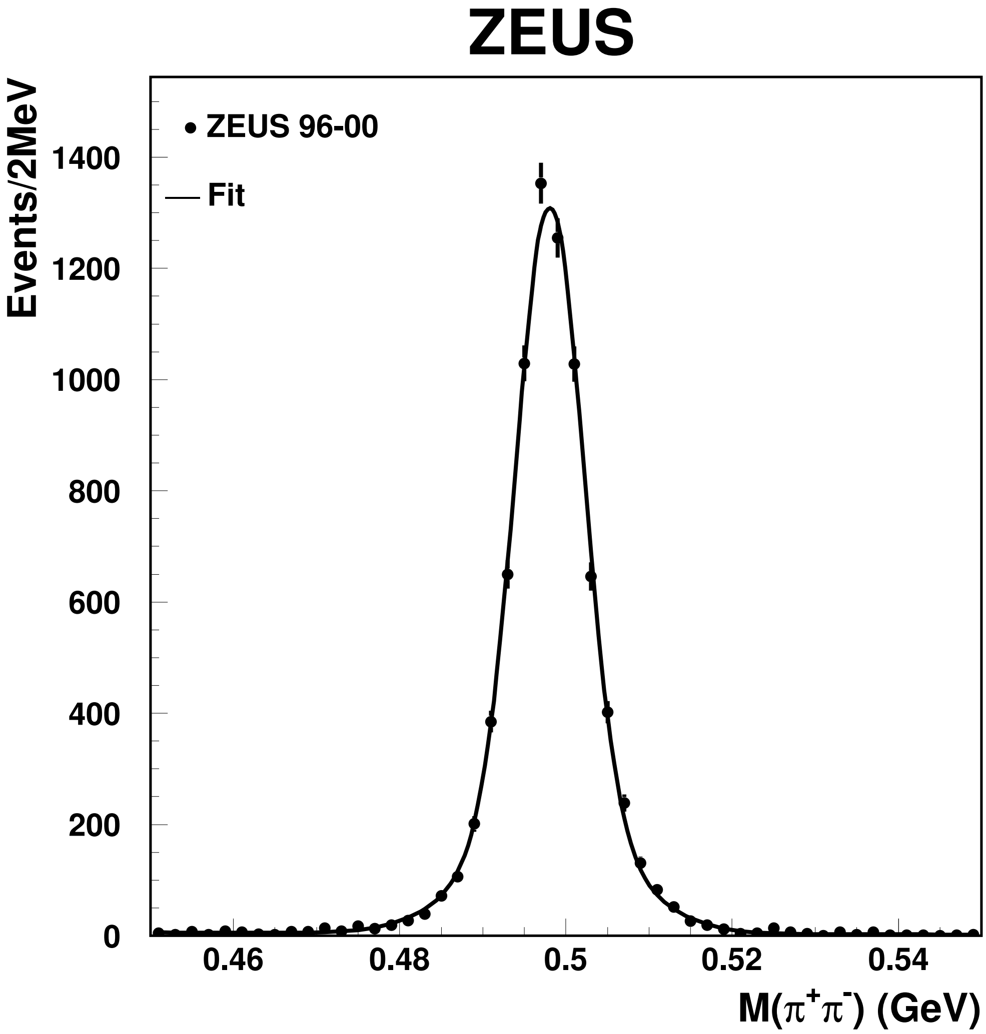

Figure 1: *The distribution of $\pi^+\pi^-$ invariant mass for events with at least two K_s^0 candidates passing all selection cuts. The solid line shows the result of a fit using one linear and two Gaussian functions.*

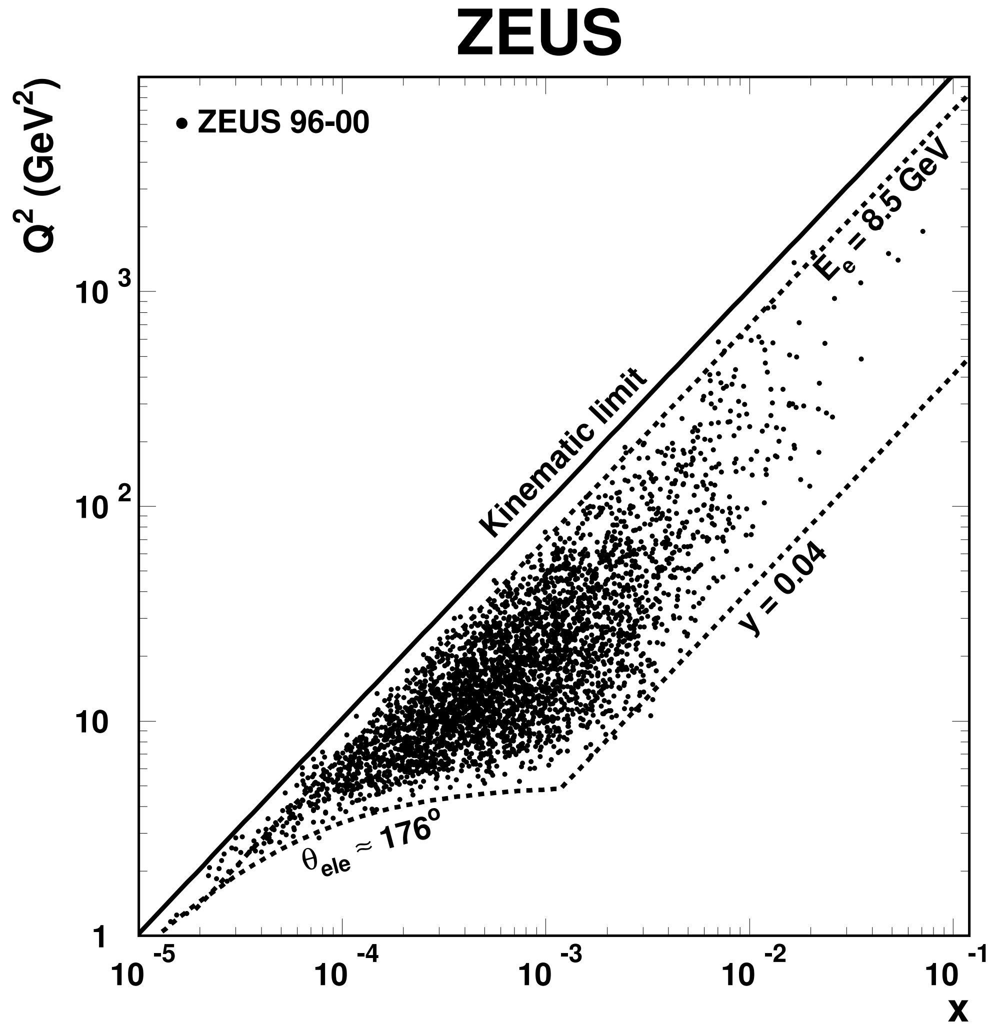

Figure 2: *The distribution in* x *and* Q^2 *of events passing all selection cuts. The dashed lines delineate approximately the kinematic region selected. The solid line indicates the kinematic limit for HERA running with 920 GeV protons.*

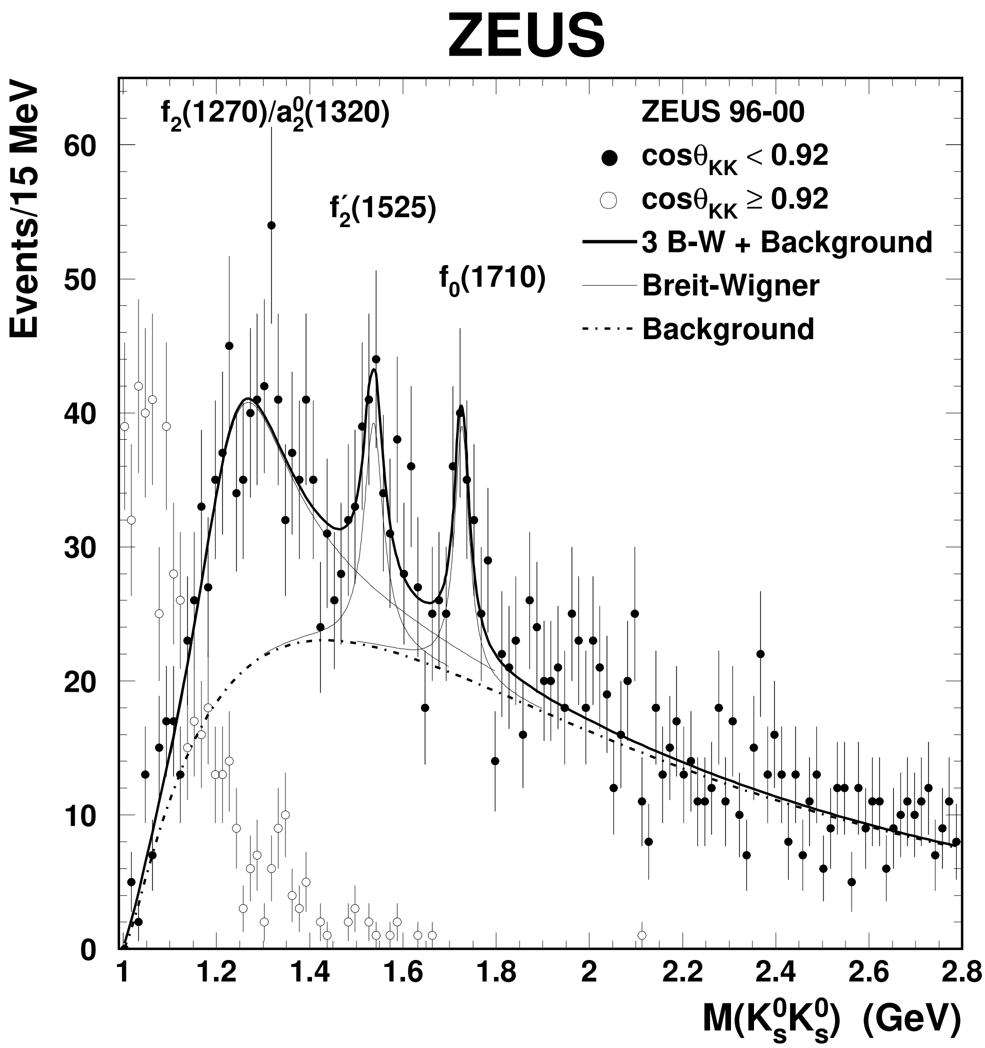

Figure 3: *The $K_s^0K_s^0$ invariant-mass spectrum for K_s^0 pair candidates with $cos\theta_{K_s^0K_s^0} < 0.92$ (filled circles). The thick solid line is the result of a fit using three Breit-Wigners (thin solid lines) and a background function (dotted-dashed line). The K_s^0 pair candidates that fail the $cos\theta_{K_s^0K_s^0} < 0.92$ cut are also shown (open circles).*